Article

Research on cantilever rock stability evaluation and early warning method based on the vibration frequency

Weinan Liu [1], Mowen Xie [1,*], Lei Zhang [1], Qingbo Li [2] and Hongfei Wang[1, 2]

[1] School of Civil and Resource Engineering, University of Science and Technology Beijing, Beijing 100083, China; grealwn@126.com (W.L.); sshi-zhang@163.com (L.Z.);
[2] Yellow River Engineering Consulting Co., Ltd. (YREC), Zhengzhou 450003, China; liqb_yrec@163.com (Q.L.); wanghf_yrec@163.com (H.W.)
* Correspondence: mowenxie@126.com

Featured Application: The method can accurately calculate the frequency of rocks in different stability. This method contributes to the real-time monitoring of dynamic changes in rock stability and early warning of rock failure based on vibration monitoring.

Abstract: For the quantitative evaluation of rock stability and early warning of rock damage based on vibration monitoring, this article analyzed the relationship between the stability of cantilevered rock and its rock bridge length, the relationship between rock bridge length and rock vibration frequency. It established a method for calculating the natural frequency of cantilevered rock. The method can use two sets of rock natural frequency and rock bridge length data obtained from field investigation to determine the natural frequency calculation formula. The rock's model experiments show that the relative error between the rocks natural frequency at the time of damage calculated based on this formula and the measured value was 4.27%. The stability change of the rock can be accurately evaluated using this formula. Compared with the displacement, which only produces sudden change before the rock is damaged, the rocks natural frequency decreases irreversibly in the early stage of rock stability decline. Therefore, monitoring the vibration frequency of rocks can warn the damage of rocks.

Keywords: cantilevered rock; rock bridge; natural frequency; rock stability

1. Introduction

Rock collapse is a kind of geological disaster with serious hazards. Accurately evaluating rocks stability and adopting suitable monitoring indicators to warn the damage of rocks are essential tasks of geological disaster prevention and control. The monitoring of slope or rock deformation can be done by satellite synthetic aperture radar remote sensing technology [1,2], ground synthetic aperture radar technology [3,4] and 3D laser scanning technology [5,6]. The slope stability can be determined by combining slope monitoring data with the numeric model calculation results [7]. However, the amount of deformation before rock collapse is small, and monitoring the rock deformation is challenging to predict the rock damage. Therefore, some scholars have studied the changes of microseismic signals [8-10], electromagnetic radiation signals [11,12] and bolt stress [13] before rock damage in addition to deformation monitoring. These indicators produce significant changes over a more extended period before rock damage than the rock deformation or displacement. Although the critical threshold of rock damage cannot be determined, the above indicators can serve as a reference for the early warning of rock failure [14,15].

In addition to the indicators mentioned above, researchers have found that the vibration frequencies of rocks and slopes under ambient noise can also reflect their stability changes [16-18]. When the rock stability increases, the resonant frequency of the rock also

rises [19]. After the slope cracking, the spectral ratio of the cracked area will have an amplification effect, and this amplification effect has an apparent polarization phenomenon [20-23]. The cliff's hazardous area can be determined with the displacement and vibration monitoring data [24]. As a result, researchers began to assess rocks stability or warn of rock damage by continuously monitoring the vibration frequency information of rocks or unstable slopes [25]. However, the studies above also failed to establish the solution method for the critical resonant frequency or the critical spectral ratio amplification coefficient of rock damage.

The vibration response of rocks under ambient noise is mainly influenced by their natural frequencies [26]. The resonant frequency values of rocks exposed to ambient vibration are the same as the natural frequency values of rocks [27]. The quantitative relationship between rock stability and its natural frequency is determined to better evaluate rock stability changes by monitoring its vibration frequency changes [28,29]. Cantilevered rocks, whose stability is controlled by the rock bridge length, are studied in this paper. The quantitative relationship between the natural frequency of cantilevered rocks and their stability is determined. The article establishes theoretical formulas for calculating the natural frequency of cantilevered rocks. These works will lay the foundation for the quantitative evaluation of rock stability and rock damage warning methods based on the natural frequency.

2. Methods

2.1. Cantilever rock stability analysis

Uneven weathering of rock strata often forms cantilevered rocks [30-32]. Unlike the tipping and sliding damage of rocks, the damage of cantilevered rocks has a strong abruptness. When cracks exist in the rock cross-section, the rock stability is mainly controlled by the rock bridge (Fig. 1a).

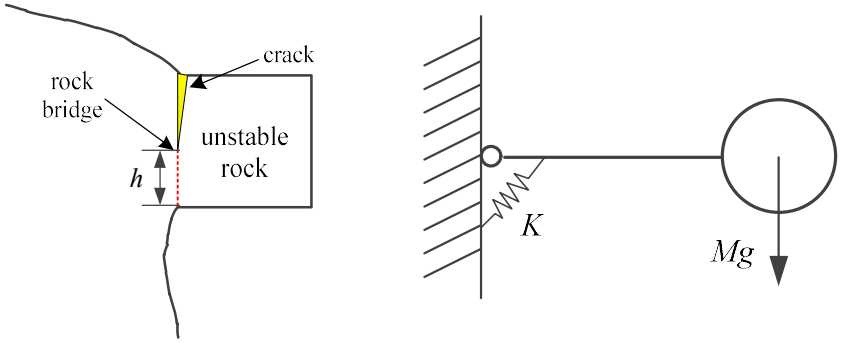

Figure 1. (**a**) Schematic diagram of a cantilevered rock; (**b**) simplified diagram of a cantilevered rock.

The maximum normal stress σ_{ma} and shear stress τ of the rock bridge can be calculated by equation (1) and equation (2). When the normal stress or shear stress exceeds the tensile strength or shear strength of the rock, it will fail.

$$\sigma_{max} = \frac{3\rho g L^2 H}{h^2} \tag{1}$$

$$\tau = \frac{\rho g H L}{h} \tag{2}$$

where ρ is the density of the rock, H is the height of the rock, L is the length of the rock, and h is the length of the rock bridge. From the formula, it can be seen that the decrease of rock bridge length h will make the increase of tensile stress and shear stress on the rock bridge. In other words, the length of the rock bridge controls the failure of the cantilevered rock. Therefore, when we analyze the stability of cantilevered rock, the rock's sta-

bility coefficient can be calculated as the ratio of the actual length of the rock bridge to its critical length.

$$F_s = \frac{h}{h_C} \tag{3}$$

where F_s is the stability coefficient of the rock, h_C is the critical length of the rock bridge calculated by equation (1) and equation (2).

2.2. Vibration characteristics of the rock

Its mass distribution and material properties control the vibration of rock. The rock bridge, which is the only constraint on the rock motion, determines the rock stability and influences the rock's vibration characteristics. By simplifying the cantilevered rock to a single degree of freedom system, the motion of the rock can be simplified to rotation around the rock bridge. Neglecting the effect of gravity, the equation of motion of the rock can be expressed as:

$$ML^2\ddot{\theta} + 4K_\theta\theta = 0 \tag{4}$$

where M is the mass of the rock, θ is the angle of rotation of the rock, and K_θ is the flexural stiffness of the rock bridge.

The natural frequency w of the rock can be calculated by equation (5).

$$w = \sqrt{\frac{4K_\theta}{ML^2}} \tag{5}$$

The flexural stiffness K_θ of the rock bridge is related to the bending mode of the rock. When the rock is rotated in the vertical plane, the flexural stiffness $K_{\theta 1}$ of the rock bridge section is calculated by equation (6). When the rock is rotated in the horizontal plane, the bending stiffness $K_{\theta 2}$ of the rock bridge section is calculated by equation (7).

$$K_{\theta 1} = \frac{EBh^3}{12} \tag{6}$$

$$K_{\theta 2} = \frac{EhB^3}{12} \tag{7}$$

where E is Young's modulus of the rock and B is the width of the rock.

Bringing equation (6) and equation (7) into equation (5), we can get the equation (Eq. 8) for the calculation of the natural frequency w_1 of rock rotation in the vertical plane and the equation (Eq. 9) for the calculation of the natural frequency w_2 of rock rotation in the horizontal plane.

$$w_1 = h^{3/2}\sqrt{\frac{E}{3\rho HL^3}} \tag{8}$$

$$w_2 = h^{1/2}\sqrt{\frac{EB^2}{3\rho HL^3}} \tag{9}$$

The shape and material properties of the rock do not change significantly in the natural environment. Therefore, the only variable in equations (8) and (9) is the rock bridge length h. The rest of the calculated parameters are unknown invariant parameters. The intrinsic frequency of the rock decreases as the length of the rock bridge decreases. Simultaneously, the decrease of the rock bridge length also leads to a decrease in rock stability. As a result, we can make the following inference: the inherent frequency of cantilevered rock will decrease with rock stability.

2.3. Formula Correction

In the above calculation process, the rock was simplified from an elastomer to a rigid body, and the rock's vibration was simplified to in-plane rotation. These simplifications must cause the difference between the theoretical formula and the actual value of the rock natural frequency. Assuming that the actual vibration frequencies of the rock in two directions are $w_{1,0}$ and $w_{2,0}$, the ratio between the calculated and actual values of the rock frequency shows a linear relationship.

$$\frac{w_1}{w_{1,0}} = a_1 h + b_1 \tag{10}$$

$$\frac{w_2}{w_{2,0}} = a_2 h + b_2 \tag{11}$$

where a_1, b_1, a_2, b_2 are correction parameters. Bringing equations (10) and (11) into equations (8) and (9), the corrected rock natural frequency is obtained as:

$$w_1 = \frac{h^{3/2}}{a_1 h + b_1}\sqrt{\frac{E}{3\rho H L^3}} \tag{12}$$

$$w_2 = \frac{h^{1/2}}{a_2 h + b_2}\sqrt{\frac{EB^2}{3\rho H L^3}} \tag{13}$$

Both Equations (12) and (13) contain the correction parameter as an unknown quantity. The correction parameters' values can be solved by bringing the measured values of the two sets of rock bridge lengths and rock natural frequencies into equations (12) and (13). From equation (3), it can be seen that its rock bridge length controls the stability of the cantilevered rock. The rock bridge length of the rock also determines its vibration frequency. When the rock bridge reaches its critical length, the rock's vibration frequency will also reach its critical value. In this way, the determination of rock stability and early warning of rock damage can be accomplished by monitoring its vibration frequency.

Different modes of rock vibrations have different values of vibration frequencies [18,33]. In this paper, two vibration forms of rock vibrating in the horizontal and vertical planes are considered when deriving the formula for rocks' vibration frequency. Therefore, when predicting the instability damage of rocks based on the natural frequency, the vibration of rocks in both directions can be monitored. The mutual correction of the monitoring results in the two directions can better determine the rock's stability changes.

3. Experiment

To analyze the relationship between the natural frequencies of cantilevered rocks and their stability, a cantilevered rock model was made using mixed materials (quartz sand, barite powder, gypsum, and water). The rock model was 60 cm long, 25 cm wide and 30 cm high. The left end of the model was fixed, and the right end was cantilevered for a length of 30 cm. The left end of the model was also fixed from above by a press (Figure 2). The vibration sensor was mounted on the rock's cantilever end, and the vibration sensor could simultaneously measure the vibration acceleration in three directions.

The cantilevered end of the rock is not subjected to any load other than gravity. The only factor affecting the rock stability in the experiment was the length of the rock bridge (depth of the crack). A crack with a depth of 4 cm was reserved when the model was cast, which was 30 cm from the rock's right end.

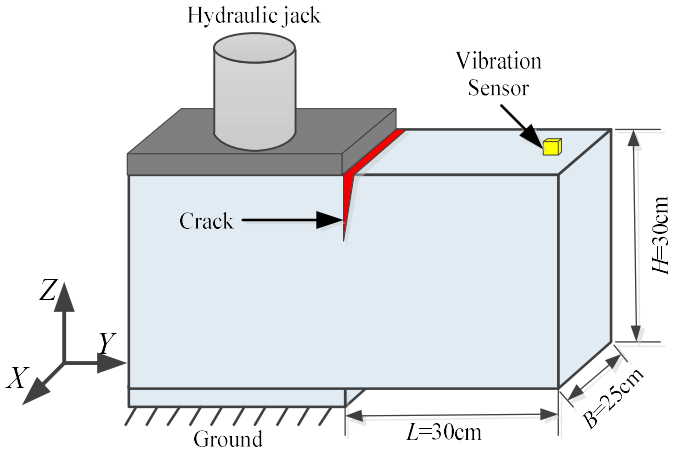

Figure 2. Schematic diagram of the experimental model

During the experiment, the rock's vibration data is measured when the crack depth is changed. The cracks were cut by a saw, and the vibration sensor started working after the cracks were cut to a specific depth. The sampling frequency of the vibration sensor is 1000 Hz. While the sensor is collecting data, the experimenter walks randomly around the model and randomly strikes the laboratory floor near the model with a hammer. The stress on the rock bridge will increase with the depth of the fracture. When the rock bridge's stress reaches the tensile strength of the model material, the rock bridge will be damaged, and the experiment will be finished.

4. Discussion

4.1. The relationship between rock bridge length and rock natural frequency

With the increase of the crack depth, the rock was destroyed at one stroke of the ground. The depth of the crack at the time of rock destruction was 17.5 cm (Fig. 3a), so the critical length of the rock bridge in this experiment was considered to be $h_c = 12.5cm$.

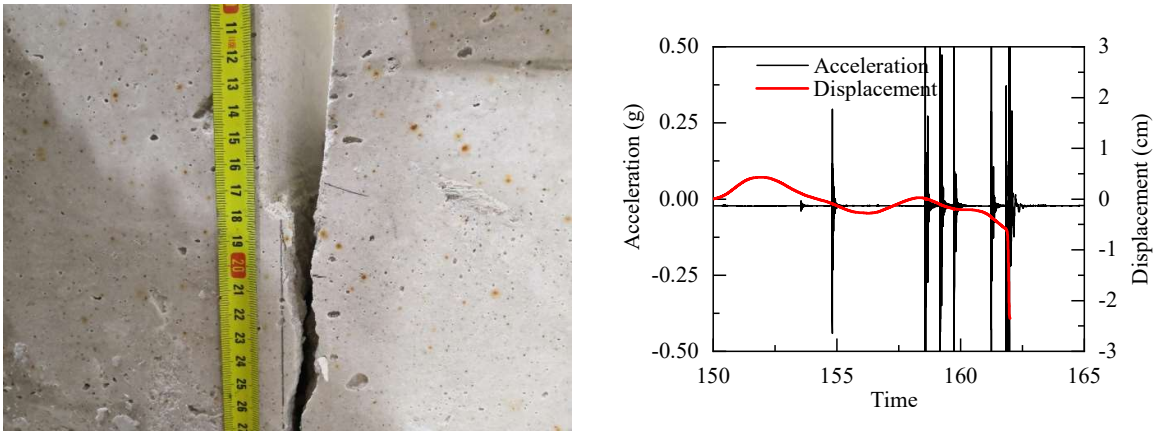

(**a**) (**b**)

Figure 3. Experimental results at rock failure: (**a**) Crack depth measurement results during rock damage; (**b**) acceleration and displacement curves of the vibration sensor in the z-direction before rock failure.

The rock was cut seven times before the rock failure, and eight sets of acceleration data of the rock under ground vibration were collected. The rock's acceleration curves were converted into frequency signals, and the spectrum curves of the rock vibration in the X and Z directions were obtained (Figure 4). Each spectrum curve showed a distinct

energy peak, and the frequency corresponding to the energy peak is a natural frequency of the rock in one model. The natural frequency of the rock model monitored by the vibration sensor in both directions decreases as the rock bridge's length decreases (Table 1). This experiment's results are consistent with the conclusions of Equations (8) and (9).

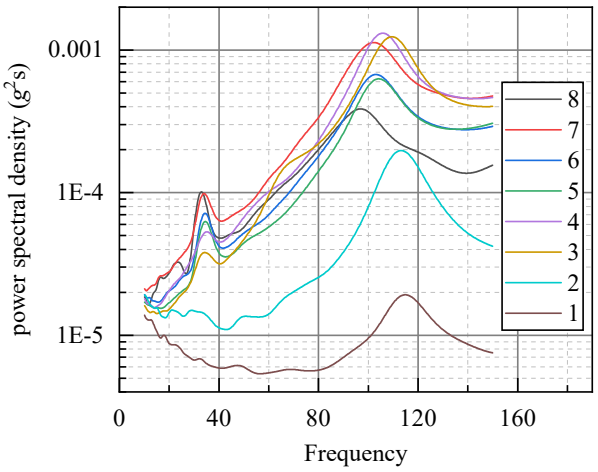

(**a**)

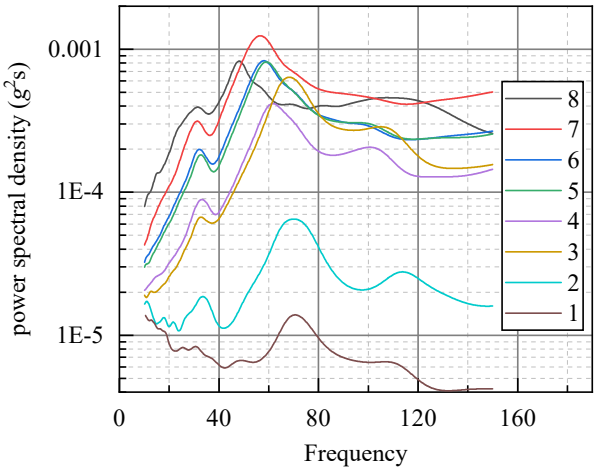

(**b**)

Figure 4. Spectral curves of rocks: (**a**) Spectrum curve of vibration sensor in X direction; (**b**) Spectrum curve of vibration sensor in Z direction.

Table 1. Rock bridge length and frequency measurement results

Number	Rock bridge length （cm）	Vibration frequency in X-direction (Hz)	Vibration frequency in Z-direction (Hz)
1	26.0	114.80	70.56
2	25.0	113.26	70.14
3	23.5	109.48	68.32
4	20.0	105.84	61.74
5	17.5	104.16	59.08
6	15.0	103.04	58.10
7	13.5	102.20	56.56
8	12.5	96.88	48.16

4.2. Calculation of rock natural frequency

Equations (12) and (13) are the theoretical formulas for calculating rock vibration frequencies, and each equation contains two correction parameters. By bringing the results of the first and second sets of experiments into Equations (12) and (13), a set of equations for calculating the rock natural frequency can be derived.

$$w_1 = \frac{h^{3/2}}{0.0098h + 0.0047} \tag{14}$$

$$w_2 = \frac{h^{1/2}}{0.0051h - 0.0002} \tag{15}$$

Equations (14) and (15) were used to calculate the natural frequencies of the rocks at the remaining six rock bridge lengths, and the differences between the calculated and measured rock natural frequencies were compared (Fig. 5). For the rock bridge length of 12.5 cm, the measured rock X-direction vibration frequency is 96.88 Hz, and its calculated result is 101.02 Hz, and the relative error between the two is about 4.27%. For the bridge length of 12.5 cm, the measured vibration frequency in the Z-direction of the rock is 48.16 Hz, and the calculated frequency is 59.67 Hz, with a relative error of about 23.90%.

Although the formula showed an error with the actual value when calculating the rock's vibration frequency in the Z direction, the formula's result was similar to the actual value when calculating the vibration frequency of the rock in the X-direction. This result proves that Eq. (14) can accurately calculate the natural frequencies of cantilevered rocks. When we measure the rock's vibration frequency, we can use equation (14) to calculate the rock bridge length of the model and then use equation (3) to calculate the stability coefficient of the rock. This is the process of rock stability quantitative evaluation based on the natural frequency, a monitorable index.

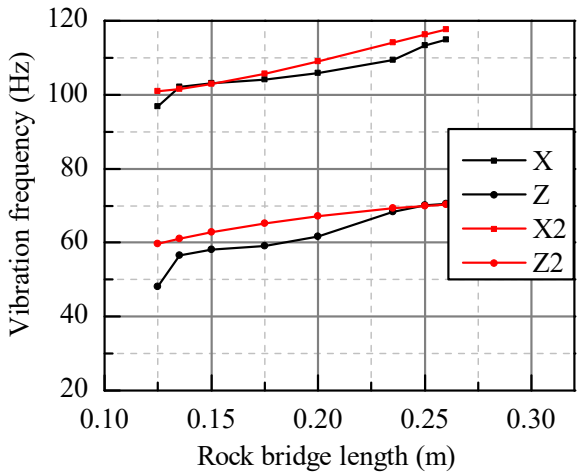

Figure 5. Calculated and measured results of the natural frequencies of the rock. In the figure: X and Z indicate the measured results of the vibration frequencies in the X and Z directions of the rock; X2 and Z2 indicate the vibration frequencies' calculated results in the X and Z directions of the rock.

A significant change in the natural frequencies of the rock occurred during the decline in the cantilevered rock's stability. During the drop of the rock bridge length from 0.26 m to 0.125 m, the natural frequencies of the rock X-direction decreased by 15.61% (measured results) and 14.2% (calculated by the formula), and the natural frequencies of the rock Z-direction decreased by 31.75% (measured results) and 15.18% (calculated by the formula). The cantilevered rock's displacement has been in fluctuation by the ground vibration during rock bridge length reduction, and it only changes abruptly when the rock bridge is broken or the rock is collapsed.

In contrast to the rock displacement, which only changes significantly when the cantilevered rock breaks (Figure 3a), the rock's vibration frequency will change irreversibly at the beginning of the rock bridge length drop (Figure 5). This phenomenon suggests that it is more effective to monitor the vibration frequency of rock than its displacement when warning its failure.

5. Conclusions

The article analyzes the influence of rock bridge length on cantilevered rock's stability, simplifies the vibration of rock as its rotation around the rock bridge in horizontal and vertical planes, establishes a simplified model of rock vibration, and gives the calculation method of rock natural frequency. Considering the errors brought by the model simplification, the article gives a correction method for the calculation formula of the rock natural frequency. The correction parameters can be calculated by bringing in two groups of actual measurements of the rock natural frequency and the length of the rock bridge. The results of both the theoretical formulation and the model experiments show that the rocks natural frequencies in both the X-direction and Z-direction decrease during the decreasing length of the cantilevered rock bridge.

The article obtained the formula for calculating the natural frequency of the cantilevered rock model. The rock natural frequency value，which calculated by this formula before rock damage, differs from the actual value by 4.27%. The experimental results show that this formula has high accuracy in evaluating the stability of rocks. The rock natural frequency will undergo a significant irreversible decrease during the stability decline of the rock. However, the rock displacement will change significantly only in a short time before its failure. This result proves that using the natural frequency index can

evaluate rock stability change and warn rock failure. Monitoring the natural frequency of rocks is more meaningful than monitoring the displacement of rocks.

Author Contributions: Conceptualization and formal analysis, W.L.; methodology and validation, M.X. and L.Z.; data curation and visualization, Q,L. and H.W.; writing, W.L. and H.W. All authors have read and agreed to the published version of the manuscript.

Funding: This research was funded by National Key Research and Development Program of China, grant number 2019YFC1509602.

Institutional Review Board Statement: Not applicable.

Informed Consent Statement: Not applicable.

Data Availability Statement: Data used in this paper are available in a public and permanent repository (http://dx.doi.org/10.17632/n3cdk898p2.1).

Conflicts of Interest: The authors declare no conflict of interest. The funders had no role in the design of the study; in the collection, analyses, or interpretation of data; in the writing of the manuscript, or in the decision to publish the results.

References

1. Manconi, A.; Kourkouli, P.; Caduff, R.; Strozzi, T.; Loew, S. Monitoring surface deformation over a failing rock slope with the ESA sentinels: Insights from Moosfluh instability, Swiss Alps. *Remote Sens.-Basel* **2018**, *10*.[http://dx.doi.org/10.3390/rs10050672]
2. Bouali, E.H.; Oommen, T.; Vitton, S.; Escobar-Wolf, R.; Brooks, C. Rockfall hazard rating system: Benefits of utilizing remote sensing. *Environmental and Engineering Geoscience* **2017**, *23*, 165-177.[http://dx.doi.org/10.2113/gseegeosci.23.3.165]
3. Woods, A.; Hendry, M.T.; Macciotta, R.; Stewart, T.; Marsh, J. GB-InSAR monitoring of vegetated and snow-covered slopes in remote mountainous environments. *Landslides* **2020**, *17*, 1713-1726.[http://dx.doi.org/10.1007/s10346-020-01408-4]
4. Dick, G.J.; Eberhardt, E.; Cabrejo-Liévano, A.G.; Stead, D.; Rose, N.D. Development of an early-warning time-of-failure analysis methodology for open-pit mine slopes utilizing ground-based slope stability radar monitoring data. *Can. Geotech. J.* **2014**, *52*, 515-529.[http://dx.doi.org/10.1139/cgj-2014-0028]
5. Ossowski, R.; Przyborski, M.; Tysiac, P. Stability Assessment of Coastal Cliffs Incorporating Laser Scanning Technology and a Numerical Analysis. *Remote Sens.-Basel* **2019**, *11*, 1951.[http://dx.doi.org/10.3390/rs11161951]
6. Liu, C.; Liu, X.; Peng, X.; Wang, E.; Wang, S. Application of 3D-DDA integrated with unmanned aerial vehicle–laser scanner (UAV-LS) photogrammetry for stability analysis of a blocky rock mass slope. *Landslides* **2019**, *16*, 1645-1661.[http://dx.doi.org/10.1007/s10346-019-01196-6]
7. Gischig, V.; Amann, F.; Moore, J.R.; Loew, S.; Eisenbeiss, H.; Stempfhuber, W. Composite rock slope kinematics at the current Randa instability, Switzerland, based on remote sensing and numerical modeling. *Eng. Geol.* **2011**, *118*, 37-53.[http://dx.doi.org/10.1016/j.enggeo.2010.11.006]
8. Luo, Z.; Wang, W.; Qin, Y.; Xiang, J. Early warning of rock mass instability based on multi-field coupling analysis and microseismic monitoring. *T. Nonferr. Metal. Soc.* **2019**, *29*, 1285-1293.[https://doi.org/10.1016/S1003-6326(19)65035-1]
9. Dou, L.; Cai, W.; Cao, A.; Guo, W. Comprehensive early warning of rock burst utilizing microseismic multi-parameter indices. *International Journal of Mining Science and Technology* **2018**, *28*, 767-774.[https://doi.org/10.1016/j.ijmst.2018.08.007]
10. Dai, F.; Li, B.; Xu, N.; Zhu, Y. Microseismic early warning of surrounding rock mass deformation in the underground powerhouse of the Houziyan hydropower station, China. *Tunn. Undergr. Sp. Tech.* **2017**, *62*, 64-74.[https://doi.org/10.1016/j.tust.2016.11.009]
11. Di, Y.; Wang, E. Rock Burst Precursor Electromagnetic Radiation Signal Recognition Method and Early Warning Application Based on Recurrent Neural Networks. *Rock Mech. Rock Eng.* **2021**, *54*, 1449-1461.[http://dx.doi.org/10.1007/s00603-020-02314-w]
12. Qiu, L.; Liu, Z.; Wang, E.; He, X.; Feng, J.; Li, B. Early-warning of rock burst in coal mine by low-frequency electromagnetic radiation. *Eng. Geol.* **2020**, *279*, 105755.[https://doi.org/10.1016/j.enggeo.2020.105755]
13. Lin, H.; Qin, J.; Chen, Y.; Xu, W.; Lei, D. Early Warning of Rock Slope Failure Based on Bolt Axial Force Monitoring. *Geotechnical and Geological Engineering* **2019**, *37*, 3985-3993.[http://dx.doi.org/10.1007/s10706-019-00887-0]
14. Feng, L.; Pazzi, V.; Intrieri, E.; Gracchi, T.; Gigli, G. Joint detection and classification of rockfalls in a microseismic monitoring network. *Geophys. J. Int.* **2020**, *222*, 2108-2120.[http://dx.doi.org/10.1093/gji/ggaa287]
15. Xu, N.W.; Dai, F.; Liang, Z.Z.; Zhou, Z.; Sha, C.; Tang, C.A. The Dynamic Evaluation of Rock Slope Stability Considering the Effects of Microseismic Damage. *Rock Mech. Rock Eng.* **2014**, *47*, 621-642.[http://dx.doi.org/10.1007/s00603-013-0432-5]
16. Lévy, C.; Baillet, L.; Jongmans, D.; Mourot, P.; Hantz, D. Dynamic response of the Chamousset rock column (Western Alps, France). *Journal of Geophysical Research* **2010**, *115*.[10.1029/2009JF001606]
17. Bottelin, P.; Jongmans, D.; Baillet, L.; Lebourg, T.; Hantz, D.; Levy, C.; Le Roux, O.; Cadet, H.; Lorier, L.; Rouiller, J.D.; Turpin, J.; Darras, L. Spectral Analysis of Prone-to-fall Rock Compartments using Ambient Vibrations. *Journal of Environmental & En-*

gineering Geophysics **2013**, *18*, 205-217.[https://doi.org/10.2113/JEEG18.4.205]
18. Bottelin, P.; Lévy, C.; Baillet, L.; Jongmans, D.; Guéguen, P. Modal and thermal analysis of Les Arches unstable rock column (Vercors massif, French Alps). *Geophys. J. Int.* **2013**, *194*, 849-858.[https://doi.org/10.1093/gji/ggt046]
19. Bottelin, P.; Baillet, L.; Larose, E.; Jongmans, D.; Hantz, D.; Brenguier, O.; Cadet, H.; Helmstetter, A. Monitoring rock reinforcement works with ambient vibrations: La Bourne case study (Vercors, France). *Eng. Geol.* **2017**, *226*, 136-145.[https://doi.org/10.1016/j.enggeo.2017.06.002]
20. Burjánek, J.; Moore, J.R.; Yugsi Molina, F.X.; Fäh, D. Instrumental evidence of normal mode rock slope vibration. *Geophys. J. Int.* **2012**, *188*, 559-569.[https://doi.org/10.1111/j.1365-246X.2011.05272.x]
21. Burjánek, J.; Gassner-Stamm, G.; Poggi, V.; Moore, J.R.; Fäh, D. Ambient vibration analysis of an unstable mountain slope. *Geophys. J. Int.* **2010**, *180*, 820-828.[https://doi.org/10.1111/j.1365-246x.2009.04451.x]
22. Kleinbrod, U.; Burjánek, J.; Fäh, D. On the seismic response of instable rock slopes based on ambient vibration recordings. *Earth, Planets and Space* **2017**, *69*.[https://doi.org/10.1186/s40623-017-0712-5]
23. Burjánek, J.; Gischig, V.; Moore, J.R.; Fäh, D. Ambient vibration characterization and monitoring of a rock slope close to collapse. *Geophys. J. Int.* **2018**, *212*, 297-310.[https://doi.org/10.1093/gji/ggx424]
24. Got, J.L.; Mourot, P.; Grangeon, J. Pre-failure behaviour of an unstable limestone cliff from displacement and seismic data. *Nat. Hazard. Earth Sys.* **2010**, *10*, 819-829.[https://doi.org/10.5194/nhess-10-819-2010]
25. Colombero, C.; Jongmans, D.; Fiolleau, S.; Valentin, J.; Baillet, L.; Bièvre, G. Seismic Noise Parameters as Indicators of Reversible Modifications in Slope Stability: A Review. *Surv. Geophys.* **2021**, *42*, 339-375.[https://doi.org/10.1007/s10712-021-09632-w]
26. Kleinbrod, U.; Burjánek, J.; Fäh, D. Ambient vibration classification of unstable rock slopes: A systematic approach. *Eng. Geol.* **2019**, *249*, 198-217.[https://doi.org/10.1016/j.enggeo.2018.12.012]
27. Mercerat, E.; Payeur, J.; Bertrand, E.; Malascrabes, M.; Pernoud, M.; Chamberland, Y. Deciphering the dynamics of a heterogeneous sea cliff using ambient vibrations: case study of the Sutta-Rocca overhang (southern Corsica, France). *Geophys. J. Int.* **2020**, *224*.[https://doi.org/10.1093/gji/ggaa465]
28. Du, Y.; Lu, Y.; Xie, M.; Jia, J. A new attempt for early warning of unstable rocks based on vibration parameters. *B. Eng. Geol. Environ.* **2020**, 1-6.[https://doi.org/10.1007/s10064-020-01839-2]
29. He, Z.; Xie, M.; Huang, Z.; Li, Y.; Sui, Z.; Lu, Y.; Golosov, A.M.; Gong, F. Experimental Hazardous Rock Block Stability Assessment Based on Vibration Feature Parameters. *Advances in Civil Engineering* **2020**, *2020*, 8837459.[https://doi.org/10.1155/2020/8837459]
30. Miščević, P.; Vlastelica, G. Impact of weathering on slope stability in soft rock mass. *Journal of Rock Mechanics and Geotechnical Engineering* **2014**, *6*, 240-250.[https://doi.org/10.1016/j.jrmge.2014.03.006]
31. Young, A.P.; Ashford, S.A. Instability investigation of cantilevered seacliffs. *Earth Surf. Proc. Land.* **2008**, *33*, 1661-1677.[https://doi.org/10.1002/esp.1636]
32. Castedo, R.; Murphy, W.; Lawrence, J.; Paredes, C. A new process–response coastal recession model of soft rock cliffs. *Geomorphology* **2012**, *177-178*, 128-143.[https://doi.org/10.1016/j.geomorph.2012.07.020]
33. Starr, A.M.; Moore, J.R.; Thorne, M.S. Ambient resonance of Mesa Arch, Canyonlands National Park, Utah. *Geophys. Res. Lett.* **2015**, *42*, 6696-6702.[https://doi.org/10.1002/2015GL064917]